Geochemical heterogeneities within the Crozet hotspot

Thomas Breton, François Nauret, Sylvain Pichat, Bertrand Moine, Manuel Moreira, Estelle F. Rose-Koga, Delphine Auclair, Chantal Bosq, Laurène-Marie Wavrant

Geochemical heterogeneities within the Crozet hotspot

Thomas Breton [a,b,*], François Nauret [a], Sylvain Pichat [b], Bertrand Moine [a,c], Manuel Moreira [d], Estelle F. Rose-Koga [a], Delphine Auclair [a], Chantal Bosq [a], Laurène-Marie Wavrant [a]

[a]Laboratoire Magmas et Volcans, Université Blaise Pascal, CNRS, IRD, 5 rue Kessler, UMR 6524, R163, F-63038 Clermont-Ferrand Cedex, France
[b]Laboratoire de Géologie de Lyon, Ecole Normale Supérieure de Lyon and Université Claude Bernard Lyon 1, CNRS UMR 5276, Université de Lyon, 46 allée d'Italie, 69007 Lyon, France
[c]Université de Lyon, Université Jean Monnet, Laboratoire Magma et Volcans, CNRS, UMR 6524, F-42023 Saint-Etienne, France
[d]Institut de Physique du Globe de Paris, Université Paris-Diderot, CNRS, UMR 7154, 4 place Jussieu, F-75252 Paris Cedex 05, France

The Crozet Plateau is a 54 Ma-old volcanic plateau that supports five islands characterized by recent volcanic manifestations that are the surface expression of a deep-mantle plume. Due to their remote location and difficult access, the Crozet Islands are poorly sampled. Both the petrological descriptions and geochemical data are scarce. Thus, the sources of the Crozet plume are still under debate. Similarly, the interactions between the Southwest Indian Ridge (SWIR) and the Crozet plume remain questioned. Here, we present a new set of isotopes (Pb, Sr, Nd and He), major and trace elements data on basalts from three islands of the Crozet Archipelago: Penguins, East, and Possession Islands. Our main purpose is to characterize the sources of the Crozet plume and to test its influence at regional scale. Two groups of lavas can be distinguished based on the isotopic data: East and Possession lavas, and Penguins lavas. Principal component analyses on our high-precision Pb isotopes data and literature data show that two mantle sources can explain most of the geochemical variability measured in Crozet lavas. A third minor contribution is however needed to fully explain the data. The entire set of isotopic compositions (Pb, Sr, Nd and He) can be explained by a mixing between three mantle sources: (1) a FOZO (Focus Zone) component, with $^{206}Pb/^{204}Pb$ higher than 19.5 and high $^{207}Pb/^{204}Pb$, $^{208}Pb/^{204}Pb$ $^{87}Sr/^{86}Sr$, $^{143}Nd/^{144}Nd$ and R/R_a ($R/R_a = \left(^3He/^4He\right)_{sample} / \left(^3He/^4He\right)_{atmosphere}$) ratios, that is mainly sampled Penguins lavas, (2) a component called "East–Possession" that is mostly sampled by the East–Possession lava group and which presents Pb, Sr and Nd isotope signatures similar to those of the Reunion–Mauritius Islands, and (3) a third minor contribution of the local Depleted MORB Mantle (DMM). The new He isotopes data on the Crozet plume allow us to propose that Crozet plume material is present in the segment of the Southwest Indian Ridge located between the Indomed (ITF) and Gallieni (GTF) transform faults. This hypothesis is confirmed by a mixing model based on trace-elements and isotopes data from the ITF–GTF segment of the SWIR and Crozet. We propose that the shallow mantle below the ITF–GTF segment of the SWIR is contaminated by deep material from the Crozet plume.

1. Introduction

Geochemical and geophysical evidence show that several segments of the Southwest Indian Ridge (SWIR) are influenced by hotspots (e.g. Meyzen et al., 2005), in particular by the Bouvet and Marion hotspots (Georgen et al., 2001; Mahoney et al., 1992). The chemical interactions between the Crozet hotspot and the SWIR (ca. 750 km apart), were described more than 20 years ago (Schilling, 1991). More recently, geophysical evidences corroborated Schilling's model: bathymetric high and mantle Bouguer anomaly low were measured between the Indomed (ITF) and Gallieni (GTF) transform faults (46°E and 52°20'E, Fig. 1A, B) (Georgen et al., 2001). Off-axis topographic and gravimetric anomalies in the ITF–GTF domain were interpreted as reflecting a melt supply

☆ **Disclosure:** Every author declares having contributed to this article. T. Breton, S. Pichat, F. Nauret, B. Moine, and E.F. Rose-Koga wrote the present article. B. Moine and F. Nauret collected the samples on Possession Island; T. Breton, B. Moine, L.-M. Wavrant and F. Nauret characterized the petrology and the mineralogy of the samples. L.-M. Wavrant, B. Moine and F. Nauret performed the major elements analyses; T. Breton and F. Nauret performed the trace elements analyses; T. Breton and S. Pichat performed the Pb isotopes analyses; C. Bosq and D. Auclair performed the Nd–Sr isotopes analyses, and M. Moreira performed the He isotopes analyses.

* Corresponding author at: Laboratoire de Géologie de Lyon, Ecole Normale Supérieure de Lyon and Université Claude Bernard Lyon 1, CNRS UMR 5276, Université de Lyon, 46 allée d'Italie, 69007 Lyon, France.
E-mail address: thomas.breton@ens-lyon.org (T. Breton).

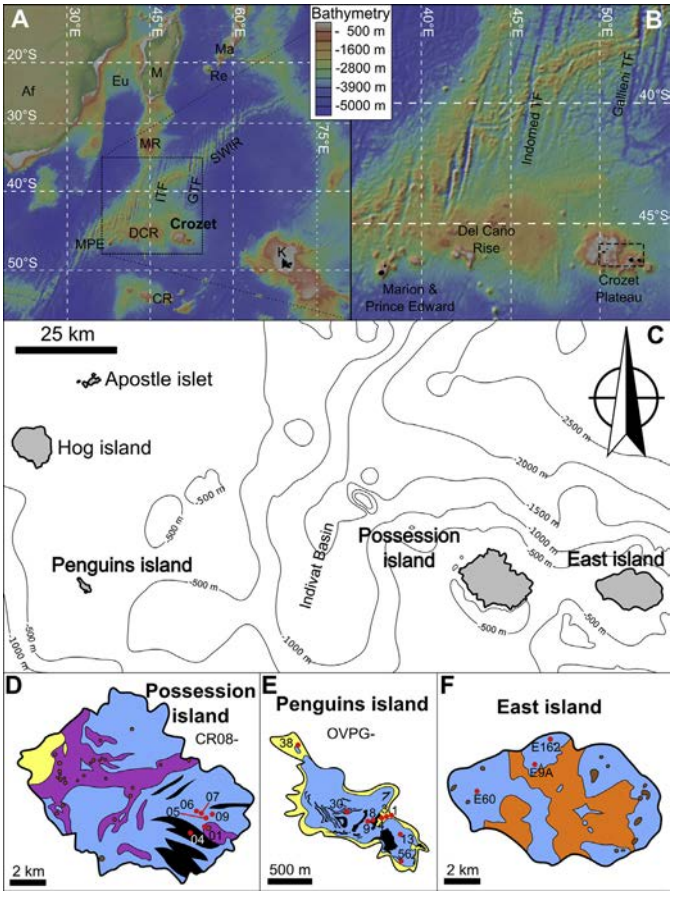

Fig. 1. The Crozet Archipelago and its geological setting. **A** – Bathymetry of the southwestern Indian Ocean (Af: Africa; CR: Conrad Rise; DCR: Del Caño Rise; Eu: Europa and Bassas da India Islands; GTF: Gallieni Transform Fault; ITF: Indomed Transform Fault; K: Kerguelen Archipelago; M: Madagascar; Ma: Mauritius Island; MPE: Marion and Prince Edward Islands; MR: Madagascar Ridge; Re: Reunion Island; SWIR: South-West Indian Ridge). **B** – Detailed bathymetry around the Crozet Plateau. **C** – The Crozet Plateau. The two groups of islands are clearly visible, separated by the 2 km-deep Indivat Basin. **D**, **E** and **F** – Simplified geological maps of the islands sampled in this study: Possession, Penguins and East Islands. Redrawn after Chevallier and Nougier (1981), Giret et al. (2002) and Lameyre and Nougier (1982) respectively. The sampling locations are represented by red dots. Pale yellow: beach levels and hyaloclastites; orange: bedded plutonic rocks; blue: hyaloclastites and interstratified lava flows (basalts, hawaiites, oceanites, ankaramites); purple: effusive strombolian volcanism; black: single lava flows; brown: recent scoria cones. **A** and **B** were built using GeoMapApp (http://www.geomapapp.org) and the Global Multi-Resolution Topography Synthesis of Ryan et al. (2009). (For interpretation of the references to color in this figure legend, the reader is referred to the web version of this article.)

anomaly that was attributed to an interaction between the SWIR and the Crozet plume (Sauter et al., 2009). This conclusion was reinforced by the observation of a shallow (75 km depth) low-velocity anomaly localized between the ITF and GTF (Sauter et al., 2009). This shallow velocity anomaly is connected to a larger anomaly at the bottom of the lithosphere that extends southward to the Conrad Rise and which is associated with high R/R_a helium data on the ITF–GTF segment of the SWIR (Gautheron et al., 2008). However, because the He isotopes signature of the Crozet Archipelago is unknown, no conclusion could be drawn on a potential interaction between the Crozet hotspot and the SWIR. Furthermore, direct and significant interactions between Crozet and the SWIR lack consensus (Meyzen et al. 2007, 2005). According to these authors the plume–ridge interaction should lead to a large increase of the $^{87}Sr/^{86}Sr$, $^{206}Pb/^{204}Pb$, $^{207}Pb/^{204}Pb$, $^{208}Pb/^{204}Pb$ ratios and a decrease of the $^{143}Nd/^{144}Nd$ ratio at the SWIR, which is not observed.

The source of the Crozet plume is also a matter of debate. Based on tomography, the Crozet and Kerguelen plumes have a common source in the deep lower mantle (Montelli et al., 2006, 2004). However, this tomographic modeling is controversial (van der Hilst and de Hoop, 2005).

The petrographic description of the Crozet Archipelago is limited to a few samples (Gunn et al., 1970). Several studies include Pb, Sr and/or Nd isotopic data (Dupré and Allègre, 1983; Giret et al., 2002; Hedge et al., 1973; Mahoney et al., 1996; Salters and White, 1998; Zhou, 1996), however the total number of analyses ($N = 27$) remains limited and often, for a given sample, one of the elements (Pb, Nd or Sr) of the isotopic dataset is not available. As a consequence, lavas from the Crozet Archipelago are poorly known compared to those of other islands in the Indian Ocean such as the Reunion or Kerguelen. The sampling of the Crozet Archipelago is extremely fragmentary because of the difficult access to these isolated and remote islands. Nonetheless, a possible isotopic heterogeneity within the Crozet plume has been mentioned by Giret et al. (2002) based on the fact that the Nd–Sr isotopic signatures of volcanic rocks from Penguins Island are distinct from those of plutonic and volcanic rocks from East Island (Zhou, 1996). Still, this observation did not allow the identification of the different mantle components involved. The Nd, Sr and Pb isotope compositions of the Afanasy-Nikitin Rise and the East and Possession Islands are distinct, hence the Crozet plume is not likely to be responsible for the formation of the Afanasy-Nikitin aseismic ridge (Mahoney et al., 1996). In fact, the lavas of East and Possession Islands have Nd, Sr and Pb isotope compositions closer to that of the Reunion and Mauritius Islands (Giret et al., 2002; Mahoney et al., 1996).

In this study, we present a new geochemical dataset for the Crozet Islands that includes major and trace elements, as well as Sr, Nd, Pb and He isotopes, and a detailed petrography of the studied samples. This dataset was obtained on new samples from the Possession, East and Penguins Islands. In particular, we present the first helium isotopes and high-precision Pb isotopes data for the Crozet Archipelago. These new data allow us to show that the basalts of the archipelago mainly derive from two deep mantle components. Mixing with small amounts of a third component, the local DMM, is invoked to fully explain the data. We also show that the geochemical signature of the SWIR between the Indomed and Gallieni transform faults can be explained by local contamination of the upper mantle by material derived from the Crozet plume.

2. Geological settings

The volcanic Crozet Archipelago is located in the Indian Ocean, 750 km southeast from the SWIR, and 1250 km WNW from the Kerguelen Islands (Fig. 1). The Crozet Archipelago is composed of five islands and islets lying on a basaltic plateau. The structural geology was described in details by Giret et al. (2003). The plateau has been dated at 54 Ma and its origin is associated with the Madagascar Plateau as both plateaus are located in symmetric positions with respect to the SWIR and present structural similarities (Goslin et al., 1981). The seafloor under the plateau is at 4000 m depth (Giret et al., 2003), between the magnetic anomalies 30 and 31 (LeMasurier et al., 1990). Gravity models indicate that the Crozet Plateau is divided into two distinct areas (Fig. 1B): (1) the Crozet Bank that supports the Crozet Archipelago is formed on old oceanic crust (Goslin and Patriat, 1984) and is interpreted as representing the recent activity of the Crozet plume (Recq et al., 1998), and (2) The Del Caño Rise that formed closer to the SWIR before the early Eocene (Goslin and Patriat, 1984).

The five islands of the Crozet Archipelago can geographically be divided into two groups. To the east, the two largest islands of the archipelago: East and Possession Islands (Fig. 1C). The Penguins

and Hog Islands, and the Apostle Islet are smaller and located about 100 km to the west. The two groups of islands are separated by the 2 km-deep Indivat Basin. The activity of the emerged volcanoes is recent, from 8.75 Ma to 0.1 Ma (Cantagrel et al., 1980), and some small volcanic cones on the islands are probably even younger (Giret et al., 2003). The late stages of activity are expressed as single lava flows and scoria cones dispersed at the surface of the islands. Seismic refraction data suggest a thick igneous crust below the Crozet Plateau down to 16.5 km (Recq et al., 1998). A positive geoid residual anomaly surrounds the Crozet Plateau, Marion and Prince-Edward Islands and the Conrad Rise (Le Roex et al., 1989). It is considered to be the expression of upper-mantle thermal-uplift of the Crozet Plateau (Sauter et al., 2009).

3. Material and methods

3.1. Samples

The samples from Possession Island (CR08-#) were collected during the DyLiOKer 2007–2008 mission. They come from the southeastern part of the island (Fig. 1D). Sample CR08-01 is from a basalt dyke in the south-eastern strombolian flow; CR08-04 is from a recent single lava flow; samples CR08-05, 06, 07 and 09 come from several lava flows interstratified in the hyaloclastites. Samples from the Penguins (OVPG#) and East (E#) Islands (Fig. 1E and F) were collected by A. Giret in 1987. The precise location of the samples is given in Appendix A1, Table A1-7 of the Supplementary material. The petrography of the studied samples is detailed in Appendix A1.

3.2. Analytical methods

We selected samples devoid of petrographic evidence for alteration. The amount of phenocrysts in the samples varied from almost none up to 40% in volume (Appendix A1, Fig. A1-3E). Minerals were analyzed by Electron Microprobe (CAMECA SX100) at the Université Blaise Pascal, Clermont-Ferrand, France. Operating conditions were 15 kV accelerating voltage, 5 nA beam current, and 10 s counting times on peak.

Whole-rock geochemical analyses were made by X-ray fluorescence (XRF, SRS4400, Bruker AXS) at the Centre SPIN, ENSM, Saint-Etienne, France, using glass discs for major elements and pressed pellets for minor elements. For major element analysis, 0.3 g of the sample was mixed with 0.3 g of $LiNO_3$ and 5.4 g of $Li_2B_4O_7$; this mixture was fused in a platinum alloy crucible at 1100 °C in a muffle furnace; a glass disc was obtained by pouring the molten mixture in a 30 mm diameter platinum mold. A routine analytical program was used for the determination of 10 oxides: SiO_2, Al_2O_3, Fe_2O_3 (total Fe as Fe_2O_3), MnO, MgO, CaO, Na_2O, K_2O, TiO_2 and P_2O_5. The "fundamental parameters" method was used to determine the matrix correction coefficients; the measured intensities were calibrated against rock standards (Appendix A1, Table A1-1b). The relative uncertainty was about 1 to 2% for the most abundant elements (Si, Al, Fe, K, Ca). The light elements (Na and Mg) and minor elements (Mn, Ti, P) were analyzed with 5% accuracy. Detection limits are in the range 0.02–0.05%. A loss on ignition (LOI) was measured by burning 1 g of sample at 800 °C during 4 hours.

For trace elements analysis, samples were dissolved in a HNO_3–HF mixture, heated for 24 hours and then evaporated. After dissolution, fluoride precipitates were dissolved with alternated additions of 7N HNO_3 and 6N HCl and evaporations. Whole-rock trace elements were obtained by solution Inductively-Coupled Plasma Mass-Spectrometry (ICP-MS, Agilent 7500, Agilent Technologies) at the Université Blaise Pascal, Clermont-Ferrand, France. A standard-sample bracketing was used: the BIR-1 standard was measured every two samples and the sample measurements where normalized by linear interpolation to the GeoReM (http://georem.mpch-mainz.gwdg.de/) preferred values of the BIR-1. Reference material BCR-2 was analyzed as unknown every four samples to assess the quality of the measurement (Appendix A1, Table A1-1a).

Strontium–Nd isotopes measurements were made by thermal ionization mass-spectrometry (TIMS, Triton, Thermo Scientific) in static mode with relay matrix rotation (virtual amplifier) on double W filaments for Nd and on single Re filament for Sr at the Laboratoire Magmas et Volcans, Clermont-Ferrand, France. The samples were leached in 1 mL HCl 1N for 15 minutes in an ultrasonic bath, followed by 45 min at 70 °C on a hotplate. After centrifugation, the supernatant was discarded and the residue was digested in 1 mL concentrated HF and 1 mL concentrated HNO_3. Chemical Sr–Nd separation were achieved using the method from Pin and Bassin (1992) and Pin et al. (1994). Sr and Nd blanks for the complete procedure were <5 ng and <200 pg, respectively. Sr and Nd isotopic measurements were (1) corrected for mass-fractionation using an exponential law and $^{86}Sr/^{88}Sr = 0.1194$ or $^{146}Nd/^{144}Nd = 0.7219$, respectively, and (2) normalized to the value of the NIST SRM 987 standard ($^{87}Sr/^{86}Sr = 0.710245$) or the value of the JNdi-1 Nd standard ($^{143}Nd/^{144}Nd = 0.512100 \pm 5$ (2σ), $n = 5$), respectively. External reproducibility was monitored by repeated analyses of NIST SRM 987 ($^{87}Sr/^{86}Sr = 0.710244 \pm 14$ (2σ), $n = 13$) for Sr and JNdi-1 Nd standard ($^{143}Nd/^{144}Nd = 0.512097 \pm 10$ (2σ), $n = 13$). These values are equal, within error margins, to the proposed values for each standard.

For Pb isotope analyses, 100 mg of powder were leached with 6N HCl for 45 min at 70 °C and rinsed with Milli-Q water before digestion in a HNO_3–HF mixture. Lead was extracted and purified by anion-exchange chromatography using a procedure adapted from Lugmair and Galer (1992). The procedure was repeated to ensure a better purification of Pb. Two procedural blanks were measured: 43 and 108 pg. Isotopic compositions were measured by Multiple-Collector ICP-MS (Nu 500 HR, Nu Instruments) at the Laboratoire de Géologie, ENS de Lyon, France, using Tl-doping to correct for instrumental mass fractionation (White et al., 2000). NBS 981 was measured every two samples to monitor machine performance. The measured ratios were subsequently normalized by linear interpolation using the values of Galer and Abouchami (1998) for NBS 981: 16.9405 for $^{206}Pb/^{204}Pb$, 15.4963 for $^{207}Pb/^{204}Pb$, 36.7219 for $^{208}Pb/^{204}Pb$. The measured 2σ standard errors on NBS 981 are 39, 57 and 77 ppm for $^{206}Pb/^{204}Pb$, $^{207}Pb/^{204}Pb$, and $^{208}Pb/^{204}Pb$, respectively. The activity of the emerged volcanoes of the Crozet Archipelago is young (8.75 Ma to 0.1 Ma, Cantagrel et al., 1980) and parent/daughter ratios are relatively low (e.g., Rb/Sr = 0.05, Sm/Nd = 0.2 and U/Pb = 0.4 in average), yielding measured isotopic ratios close to initial isotopic ratios. Thus in the following discussion, the Pb isotopic data are not corrected from radioactive decay.

Helium concentrations and isotopic ratios were determined using noble gas mass-spectrometer (Noblesse, Nu Instruments) at the Institut de Physique du Globe de Paris, France. Between 0.3 and 1.1 g of olivine crystals were picked from the samples and subsequently cleaned with distilled water and ethanol in an ultrasonic bath. After a night of heating at 150 °C under vacuum, they were crushed using a magnetic ball moved with a magnet and the gas was purified using a titanium getter at 800 °C and a SAES getter at room temperature. Helium and neon were separated at 70 K and introduced independently in the mass spectrometer. Typical ^4He blank is 10^{-10} ccSTP. The detailed analytical procedure is given in Moreira et al. (1995).

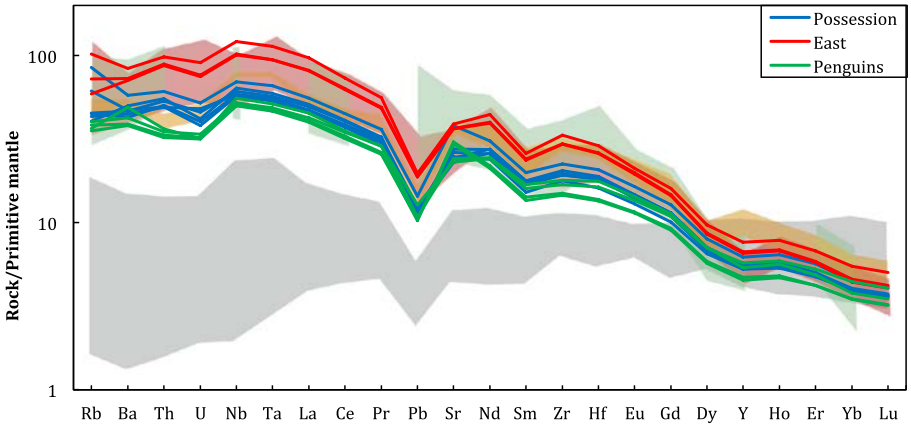

Fig. 2. Trace elements patterns normalized to primitive mantle (Hofmann, 1988) of the analyzed samples of Possession Island (blue lines), East Island (red lines) and Penguins Island (green lines). The red and green fields correspond respectively to data from East Island and Penguins Island from previous studies (Giret et al., 2002; Zhou, 1996). The grey field corresponds to data for the SWIR (http://www.petdb.org/, references listed in Appendix A4). The orange field represents the data for Marion and Prince Edward (Janney et al., 2005). (For interpretation of the references to color in this figure legend, the reader is referred to the web version of this article.)

4. Results

4.1. Major elements

Whole-rock major element compositions are presented in Appendix A1, Table A1-1a. In a Total Alkali vs. Silica (TAS) diagram, the studied rocks plot in the fields of basalts, picro-basalts and basanites (Appendix A1, Fig. A1-2). As most of the studied alkali basalts are very rich in olivine and clinopyroxene crystals, they belong to the ankaramite basanite subgroup according to the IUGS recommendations (Gunn et al., 1970; Le Maitre et al., 1989). Diagrams presenting major elements oxides vs. MgO are available in Appendix A1, Fig. A1-3. This figure also presents the evolution of the phenocrysts abundance as a function of MgO.

Unambiguous trends are clearly identified in the Crozet basalt. The basalt from the three studied islands cannot be distinguished on the basis of the major elements compositions alone, as the samples from Possession Island, East Island and Penguins Island overlap in the major elements diagrams. The compositions observed in the studied rocks are in agreement with the results from previous studies (Gunn et al., 1970; Zhou, 1996). MgO varies from 20 to 2 wt% and falls down to 0.2 in the most differentiated samples of the islands (trachytes and rhyolites). With the increasing MgO, one can observe a decrease in SiO_2, Al_2O_3 and alkali ($Na_2O + K_2O$), and an increase in FeO and CaO. TiO_2 increases for MgO < 6 and subsequently decreases dramatically. Noteworthy, SiO_2, FeO, CaO and to a lesser extent $Na_2O + K_2O$ show an important change of slope when MgO exceeds this same value. The variability observed in MgO appears to be related both to differentiation and to the phenocrysts abundance in the rocks: the aphyric rocks present the highest $Na_2O + K_2O$ content. The calculated CIPW (Appendix A1, Table A1-6) norms of the samples show that all are nepheline-normative and are tephritic phonolites according to the Streckeisen classification.

4.2. Trace elements

Trace element concentrations are reported in Appendix A1, Table A1-1a. The lavas from the Crozet Archipelago have similar patterns, coherent with an Oceanic Island Basalt (OIB) source: they are enriched in incompatible trace elements compared to MORBs and are depleted in HREE relative to LREE (Fig. 2). Moreover, they show typical OIB trace elements ratios, for instance a Ba/Nb ratio of 7.5 ± 1.0, and a Ba/Ce ratio equal to 4.5 ± 0.6 (Halliday et al., 1995). They all present similar characteristics such as a slight depletion in Rb, Ba, Th, U relative to Nb and Ta. Their Nb/U (44.3 ± 8.2) and Ce/Pb (29.8 ± 4.7) are typical of mantle melts (Hofmann et al., 1986) although the Nb/U are on the lower-end of the OIB range (52 ± 15) (Hofmann, 2007). High Dy/Yb ratios (2.5–2.8) suggest the presence of residual garnet in the source. There is however a shift of the abundances of the most incompatible elements between the three islands with higher values for East relative to Possession and Penguins. In particular, lavas from East Island are enriched in Ba (431–508 ppm), Th (7.10–8.02 ppm) and Nb (62.3–75.8 ppm) compared to Penguins Island lavas (Ba = 234–296 ppm, Th = 2.67–2.95 ppm and Nb = 31.5–34.4 ppm).

4.3. Isotope compositions

Isotope compositions in Nd, Sr, Pb and He are reported in Table 1 and Figs. 3 and 5. East and Possession Islands have homogeneous Sr isotopic ratios (0.704029 to 0.704488) and $^{143}Nd/^{144}Nd$ (0.512822 to 0.512857) (Fig. 3A). Our Sr and Nd isotopic data are in agreement with the results of previous studies for both East Island ($^{87}Sr/^{86}Sr$ = 0.7039–0.7045 and $^{143}Nd/^{144}Nd$ = 0.51274–0.51286) (Giret et al., 2002; Mahoney et al., 1996; Zhou, 1996) and Possession Island ($^{87}Sr/^{86}Sr$ = 0.7040–0.7041 and $^{143}Nd/^{144}Nd$ = 0.51283–0.51285) (Mahoney et al., 1996). Samples from Penguins Island display less radiogenic Sr isotope ratios (0.703211 to 0.703324) than the other islands, and more radiogenic $^{143}Nd/^{144}Nd$ (0.512931 to 0.512960, Fig. 3A).

The same two groups of islands can be distinguished with Pb isotopic compositions. Possession and East Island lavas ($^{206}Pb/^{204}Pb$ = 18.8861–19.1550, $^{207}Pb/^{204}Pb$ = 15.5821–15.6063,$^{208}Pb/^{204}Pb$ = 38.9717–39.1976) define a linear correlation in each of the $^{207}Pb/^{204}Pb$ vs. $^{206}Pb/^{204}Pb$ ($r^2 = 0.79$) and the $^{208}Pb/^{204}Pb$ vs. $^{206}Pb/^{204}Pb$ ($r^2 = 0.74$) spaces (Figs. 3B, C). Our Pb data overlap those from the literature (Hedge et al., 1973; Mahoney et al., 1996; Salters and White, 1998; Zhou, 1996). Penguins Island lavas are more radiogenic than those of the other groups of islands with $^{206}Pb/^{204}Pb$ of 19.2239–19.6468, $^{207}Pb/^{204}Pb$ of 15.6072–15.6325, and $^{208}Pb/^{204}Pb$ of 39.0900–39.3506. The samples define a clear linear correlation in each of the $^{207}Pb/^{204}Pb$ vs. $^{206}Pb/^{204}Pb$ and the $^{208}Pb/^{204}Pb$ vs. $^{206}Pb/^{204}Pb$ spaces ($r^2 = 0.91$ and 0.93, respectively, Figs. 3B, C).

The two groups of islands are also distinct in He isotopic compositions: the East and Possession lavas have less primitive R/R_a (8.2 ± 1.2, $N = 5$ with $R/R_a = \left(^3He/^4He\right)_{sample} / \left(^3He/^4He\right)_{atmosphere}$) than those of Penguins (13.4 ± 0.5, $N = 3$). The high Penguins Island ratios are similar to those of the Reunion Island (R/R_a be-

Table 1
Nd, Sr, Pb and He isotopic compositions of the Crozet samples.

Sample	Island	$^{87}Si/^{86}Sr$	$^{143}Nd/^{144}Nd$	$^{206}Pb/^{204}Pb$	$^{207}Pb/^{204}Pb$	$^{208}Pb/^{204}Pb$	$[^4He]^a$ (ccSTP/g)	$(R/R_a)^{(1)}$
CR08-01	Possession	0.704029 ± 5	0.512852 ± 7	18.8948 ± 9	15.5891 ± 8	39.0406 ± 25	7.58×10^{-9}	8.20 ± 0.21
CR08-04	Possession	0.704089 ± 4	0.512857 ± 3	19.1550 ± 13	15.6063 ± 12	39.1976 ± 35	8.52×10^{-9}	8.79 ± 0.17
CR08-05	Possession	0.704307 ± 3	0.512833 ± 3	19.0049 ± 9	15.5980 ± 9	39.1268 ± 23	2.68×10^{-8}	8.75 ± 0.10
CR08-06	Possession	0.704109 ± 4	0.512849 ± 9	18.9915 ± 12	15.5947 ± 10	39.0848 ± 29	2.72×10^{-8}	7.88 ± 0.09
CR08-07	Possession	0.704306 ± 3	0.512853 ± 3	18.9865 ± 11	15.5898 ± 10	39.0693 ± 27	6.47×10^{-9}	7.94 ± 0.22
CR08-09	Possession	0.704488 ± 4	0.512855 ± 3	18.8861 ± 9	15.5821 ± 8	38.9717 ± 27	8.19×10^{-9}	7.41 ± 0.15
E60	East	0.704038 ± 3	0.512831 ± 2	18.8956 ± 11	15.5838 ± 8	39.0433 ± 24	–	–
E162	East	0.704047 ± 3	0.512824 ± 3	18.8973 ± 10	15.5844 ± 10	39.0483 ± 26	–	–
E9A	East	0.704170 ± 3	0.512822 ± 4	18.9647 ± 11	15.5864 ± 10	39.1495 ± 29	2.74×10^{-7}	8.41 ± 0.07
OVPG1	Penguins	0.703272 ± 7	0.512932 ± 6	–	–	–	–	–
OVPG3	Penguins	0.703227 ± 9	0.512954 ± 7	19.3241 ± 10	15.6072 ± 9	39.1078 ± 24	–	–
OVPG4	Penguins	0.703324 ± 7	0.512947 ± 7	19.2239 ± 13	15.6112 ± 10	39.0900 ± 28	–	–
OVPG8	Penguins	0.703230 ± 7	0.512938 ± 11	–	–	–	1.94×10^{-8}	13.98 ± 0.14
OVPG-9	Penguins	–	–	19.3586 ± 20	15.6170 ± 16	39.1855 ± 40	1.28×10^{-8}	13.71 ± 0.16
OVPG-13	Penguins	0.703284 ± 6	0.512953 ± 13	19.6339 ± 12	15.6325 ± 10	39.3506 ± 27	3.33×10^{-9}	13.19 ± 0.16
OVPG23	Penguins	0.703234 ± 7	0.512960 ± 5	19.6086 ± 8	15.6302 ± 8	39.3287 ± 24	–	–
OVPG30	Penguins	0.703265 ± 7	0.512931 ± 8	19.6054 ± 4	15.6320 ± 4	39.3060 ± 13	–	–
OVPG-38	Penguins	–	–	19.3145 ± 25	15.6125 ± 20	39.1139 ± 53	4.73×10^{-8}	13.34 ± 0.12
OVPG48	Penguins	0.703211 ± 7	0.512952 ± 5	19.6468 ± 14	15.6295 ± 12	39.2797 ± 34	–	–
OVPG56	Penguins	0.703219 ± 8	0.512949 ± 5	19.2246 ± 7	15.6078 ± 7	38.9384 ± 16		

(1) He isotopes were measured on olivine. See Material and methods section for details.

tween 11.5 and 13.3, Graham et al., 1990; Hopp and Trieloff, 2005, and references therein) or other plumes with deep-mantle origin, like Hawaii or the Galapagos Islands (Farley and Neroda, 1998; Hofmann et al., 2011, and references therein).

In order to decipher relationships between Crozet and other volcanic islands of the Southwestern Indian Ocean, we compare the Crozet Archipelago lavas to those from the neighboring hotspots (Fig. 3). In the $^{87}Sr/^{86}Sr$ vs. $^{143}Nd/^{144}Nd$ space and in the Pb–Pb isotope spaces, East and Possession samples have isotopic compositions similar to those of the Reunion and Mauritius Islands. In contrast, Penguins Island samples have $^{87}Sr/^{86}Sr$ and $^{143}Nd/^{144}Nd$ compositions close to those of both Marion and Prince Edward, and Comoros while their Pb–Pb isotope compositions solely plot in the field defined by Comoros lavas.

5. Discussion

5.1. Fractional crystallization and crystal accumulation

Major elements compositions have been previously reported for East Island by Gunn et al. (1970). Their variations among the Crozet lava series were interpreted as resulting from fractional crystallization of olivine and pyroxene, plus minor amounts of chromian spinel, from alkaline parent magma. Our samples display variations of major elements composition similar to those reported by Gunn et al. (1970) for East Island. Hence, the magmatic processes involved in the formation of all the studied Crozet lavas are likely to be similar. In particular, addition/subtraction of olivine and pyroxene phenocrysts to/from a common parent magma is sufficient to explain the observed major elements compositional variations. Still, a variation in the degree of partial melting of the mantle source could produce similar variations in the major elements composition.

Trace elements variations can provide independent support for the role of partial melting and crystal extraction/accumulation in the compositional variations of the Crozet lavas. The trace elements patterns of the three islands are similar (Fig. 2), however, the East Island lavas are more enriched than those of Possession and Penguins Islands. Both variation in the degree of partial melting (Giret et al., 2002) and/or accumulation olivine and pyroxene in the erupted lava (Gunn et al., 1970) could lead to the decrease of trace element concentrations observed in the Crozet lavas. Both processes, either an increase of the degree of partial melting or an addition of olivine and clinopyroxene crystals, tend to dilute the incompatible trace elements. In the case of the addition of ferromagnesian crystals, it is explained by the crystal–liquid partition coefficient of those elements being well below unity.

Scandium and Ni have a high affinity for the clinopyroxene and olivine, respectively. Thus, the crystallization and extraction of large amounts of clinopyroxene and olivine during the magma ascent could explain that the East Island lavas, which have the lowest amount of phenocrysts (Appendix A2, Table A2-1), have lower Sc and Ni concentrations than that of Possession and Penguins Islands (Appendix A1, Table A1-1a).

The study of the evolution of the concentration incompatible trace elements, such as La, as a function of the amount of clinopyroxene and olivine phenocrysts can help us to discriminate between partial melting and crystal extraction/addition (Appendix A2, Fig. A2-1). There is a clear negative linear correlation that illustrates the dilution phenomenon of the incompatible trace elements by increasing the amount of phenocrysts, which goes in favor of the accumulation hypothesis previously proposed by Gunn et al. (1970). Thus, the East Island lavas studied here differ from those of Possession and Penguins Islands in terms of trace element concentration because the last two accumulated olivine and pyroxene phenocrysts, thus diluting the trace elements in the resulting basalt. This is confirmed by the negative correlations of CaO/Al_2O_3 vs. incompatible element concentrations.

5.2. Characterization of the Crozet mantle source

Lavas from the Penguins Island have Sr, Nd and Pb isotopes signatures distinct from those of the East and Possession Islands (Fig. 3). Similarly, the R/R_a ratio (13.4 ± 0.5, $N = 3$) of Penguins lavas is higher than those of East and Possession (8.2 ± 1.2, $N = 5$) (Table 1). In addition, Penguins lavas present a depletion in Th relative to the other islands (Fig. 2). This depletion is unlikely to be due to an analytical artifact that would affect the samples randomly. Thus, the depletion in Th of the Penguin lavas is likely a characteristic of their mantle source. Hence, both isotopes and trace elements suggest different lava sources for the two groups of islands rather than an influence of crystallization or melting processes.

In order to determine the number of mantle sources for Crozet, we performed Principal Component Analyses (PCA) on the Pb isotopic compositions of Crozet lavas (Figs. 4A, B)). Details concerning the PCA are provided in Appendix A3. In the literature, the source materials of magmas are often referred to as component as are

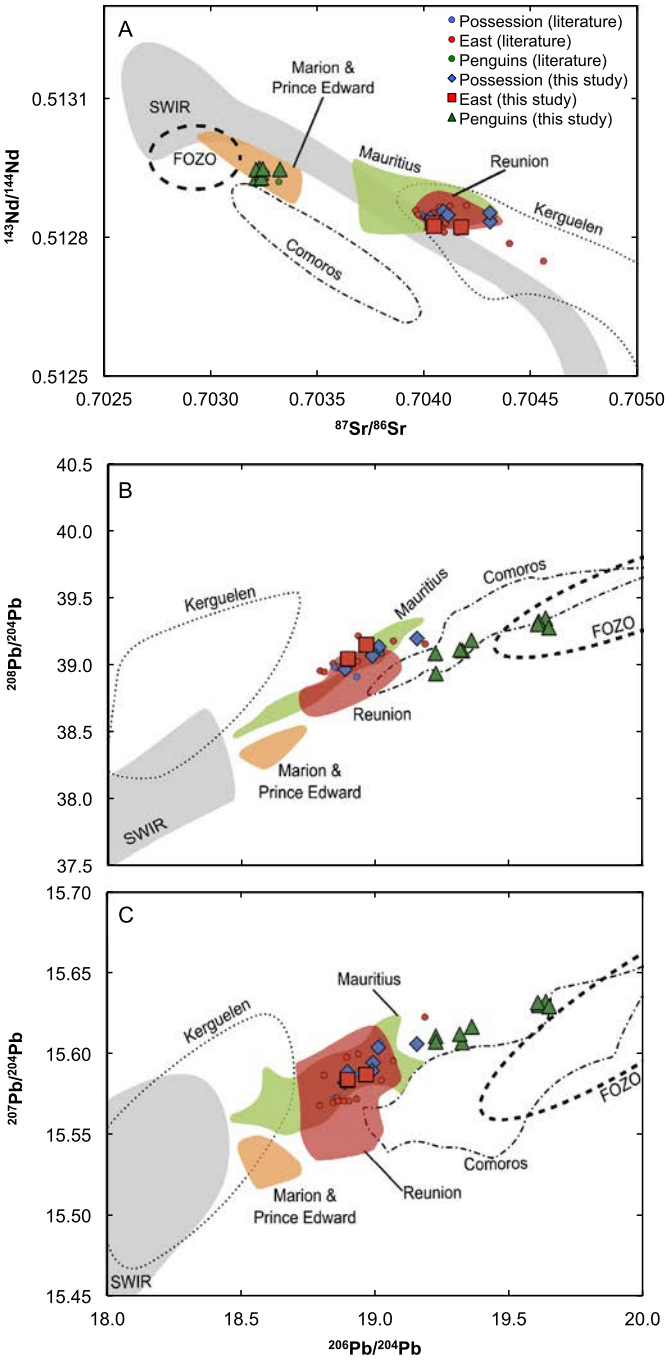

Fig. 3. **A** – $^{143}Nd/^{144}Nd$ vs. $^{87}Sr/^{86}Sr$, **B** – and **C** – $^{208}Pb/^{204}Pb$ and $^{207}Pb/^{204}Pb$ vs. $^{206}Pb/^{204}Pb$, for the studied samples. Possession, East and Penguins Islands data are from this study (Table 1) and from the literature (Giret et al., 2002; Mahoney et al., 1996; Zhou, 1996). Error bars are smaller than the symbols. SWIR MORB data are from the PetDB database (http://www.petdb.org/). Data for the Kerguelen, Comoros, Reunion and Mauritius Islands are from the GeoROC database (http://georoc.mpch-mainz.gwdg.de/) (references are listed in Appendix A4). Data for the Marion Island are from the GeoROC database and Le Roex et al. (2012). The FOZO fields are drawn after Stracke et al. (2005). No renormalization of the Pb data was performed because the effect would be insignificant compared to the overall dispersion of the data.

the orthogonal coordinates produced by PCA. To avoid ambiguities between the two terminologies, we will refer to orthogonal coordinates produced by PCA as 'principal components'. The first and second principal components account for 89.6% and 7.4% of the variance while the third principal component only accounts for 3.0% of the variance (Fig. 4A). If we only take into account our

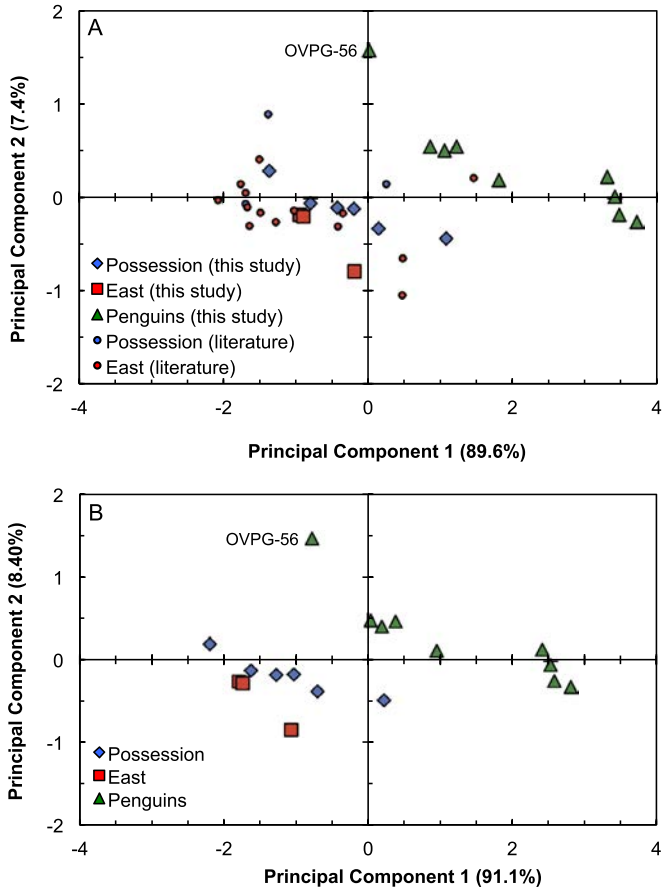

Fig. 4. Principal Component Analysis **A** – applied to all the Crozet Pb isotopic data (this study and data from the literature) and **B** – restricted to the Crozet high-precision Pb isotopic data from this study.

high-precision Pb data, the dominance of the first principal component is even more striking (91.1%) and the contribution of the third principal component then almost vanishes (0.5%) (Fig. 4B). Thus, two mantle sources explain most of the variability but a third minor source is involved. In the PCA diagrams (Figs. 4A, B), East and Possession lavas plot along the axis of the first principal component and to the right of the axis of the second principal component, and most of the Penguins lavas plot along the axis of the first principal component and to the left of the axis of the second principal component. A hint of the third mantle source is visible as the samples are not perfectly aligned along the first principal component but scattered by the second principal component (e.g. sample OVPG-56).

Because Pb–Pb isotopes plots (Figs. 3B, C) alone cannot always be discriminative between potential mantle source end-members and provide ambiguous relationships between samples and sources, we have based the following discussion on Sr and Nd vs. Pb isotopes plots to determine the three mantle sources involved in Crozet (Fig. 5). The results in both the $^{87}Sr/^{86}Sr$ vs. $^{206}Pb/^{204}Pb$ and $^{143}Nd/^{144}Nd$ vs. $^{206}Pb/^{204}Pb$ spaces are similar to those of the PCA on Pb isotopes: the Crozet lavas form two main groups, one with the East and Possession Island samples and the other with the Penguins Island samples. Our new East and Possession Island isotopic data plot within the field defined previously by Mahoney et al. (1996) and Zhou (1996) (Fig. 5). Our new data show that Penguins Island lava form a distinct group with lower $^{87}Sr/^{86}Sr$, higher $^{206}Pb/^{204}Pb$, and higher $^{143}Nd/^{144}Nd$ than the East and Possession group. Thus, the Crozet plume appears to sample several mantle sources similar to what is ob-

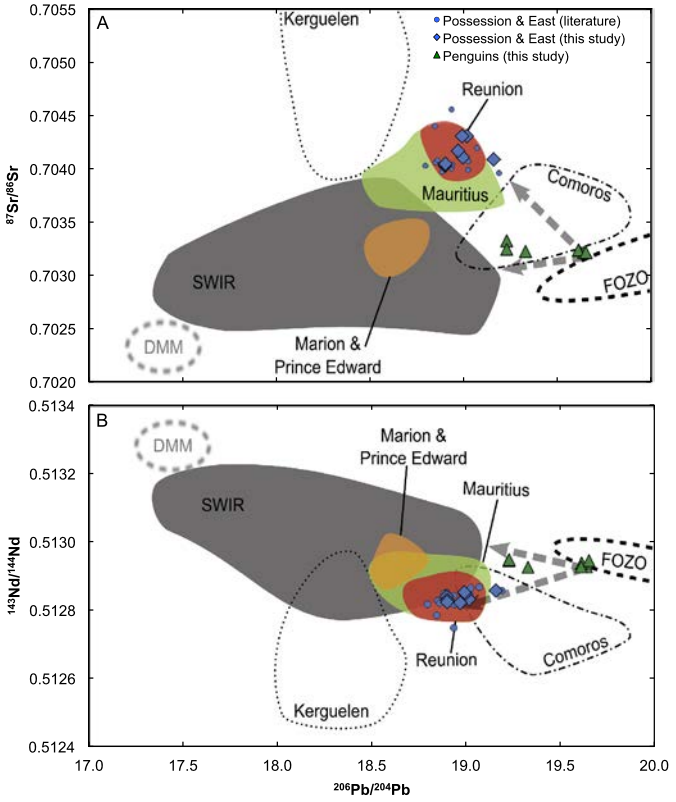

Fig. 5. A – $^{87}Sr/^{86}Sr$ vs. $^{206}Pb/^{204}Pb$ and **B** – $^{143}Nd/^{144}Nd$ vs. $^{206}Pb/^{204}Pb$ of the Crozet samples. Symbols are the same as in Fig. 3. Dashed arrows highlight that at least 3 mantle components – FOZO, DMM, and Reunion–Mauritius-like (see text for details) – are required to explain the isotope variability within the Crozet hotspot. The FOZO field is the one defined by Stracke et al. (2005). The DMM field is drawn after the D-DMM defined by Workman and Hart (2005).

served for the Hawaii hotspot for example (Abouchami et al., 2000; Blichert-Toft and Albarède, 2009; Eisele et al., 2003; Fekiacova et al., 2007).

Four samples from the Penguins Island (OVPG-13, 23, 30, 48) present characteristics similar to those of the FOZO (Focus Zone) component with $^{206}Pb/^{204}Pb$ higher than 19.50, moderately high $^{87}Sr/^{86}Sr$ and $^{143}Nd/^{144}Nd$ ratios (Fig. 5). FOZO was initially defined by Hart et al. (1992), but we use the more recent Pb, Sr and Nd isotope values given by Stracke et al. (2005). Furthermore, the high R/R_a ratio (helium composition) of the Penguins Island samples (13.4 ± 0.5, Table 1) are in good agreement with the unradiogenic values of the FOZO component (Farley et al., 1992; Hanan and Graham, 1996; Hart et al., 1992). These observations suggest that one of the mantle-sources sampled by the Crozet basalts is a FOZO-like component and is best preserved in, or mostly sampled by, the Penguins Island lavas.

The East and Possession Islands lava group have Pb, Nd and Sr isotope signatures similar to those of the Reunion and Mauritius hotspots (Fig. 5). This suggests that, despite the distance between the islands (~3000 km), the Reunion plume and a part of the Crozet plume sample either the same mantle reservoir or a reservoir with similar chemical characteristics. However, in a graph reporting $^{143}Nd/^{144}Nd$ or $^{87}Sr/^{86}Sr$ versus $^{206}Pb/^{204}Pb$, East and Possession Island lavas are also on a tie line between the FOZO-like end-member defined by the Penguins lava group and the Kerguelen data (Fig. 5). Thus the isotopic signatures of the East and Possession lava group could also be interpreted as reflecting a contribution of a Kerguelen mantle source to the Crozet hotspot. This hypothesis is supported by the tomography results of Montelli et al. (2004) but the results from this tomographic modeling are controversial (van der Hilst and de Hoop, 2005).

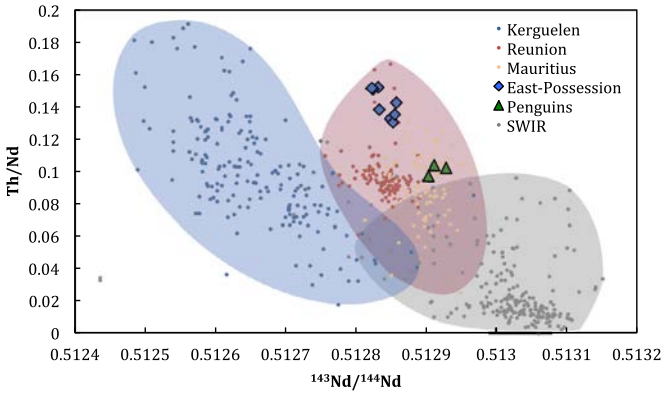

Fig. 6. Th/Nd vs. $^{143}Nd/^{144}Nd$. Data for Kerguelen, Reunion and Mauritius are from the GeoROC database (http://georoc.mpch-mainz.gwdg.de/), and data for the SWIR MORBs are from the PetDB database (http://www.petdb.org/). References are listed in Appendix A4.

To discriminate between the two hypotheses presented above, we use a Th/Nd vs. $^{143}Nd/^{144}Nd$ diagram (Fig. 6). In this diagram, binary mixing processes result in linear fields as both axes have Nd at the denominator (Langmuir et al., 1978; Vollmer, 1976). If the hypothesis of a mixing between the Kerguelen mantle source and a FOZO-like end-member is true, the Penguins Island samples and the East–Possession Islands samples should lie on a linear array pointing towards the Kerguelen field. We can reject this hypothesis because the trend defined by the Crozet samples is parallel to that of Kerguelen and lie in the field defined by the Reunion–Mauritius samples. Thus, we can conclude that Crozet samples represent a mixing between a FOZO-like and a Reunion–Mauritius-like mantle sources. Crozet and Reunion–Mauritius lavas appear to sample a similar mantle source or, at least, a region of the mantle with similar geochemical characteristics, distinct from that of the Kerguelen Archipelago. As (1) we have no further evidence about the source being the same for Crozet and Reunion–Mauritius, and as (2) the distance between Crozet and Reunion–Mauritius Islands is of ca. 3000 km, we choose to call this second mantle source the E–P (for East–Possession) component.

At least one sample from Possession Island (CR08-04) may result from the mixing of this E–P component and the FOZO component, as it plots between the FOZO field and the field defined by East–Possession lavas in $^{87}Sr/^{86}Sr$ vs. $^{206}Pb/^{204}Pb$ or $^{143}Nd/^{144}Nd$ vs. $^{206}Pb/^{204}Pb$ diagrams (Fig. 5).

Three samples from Penguins Island (OVPG-3, -4 and -56) cannot be explained by a binary mixing between the two mantle sources defined above (Fig. 5). The samples plot between the FOZO field and a field defined by SWIR MORBs. We interpret this trend as reflecting a mixing between the FOZO-like source and a Depleted MORB Mantle (DMM) end-member.

Our new data on the Penguins Island show that three mantle sources are required to explain the geochemical variations within the Crozet hotspot. Two of them are sampled in large proportions in the Crozet lavas: a FOZO-like component and an E–P (Reunion-like) component. These components are heterogeneously sampled within the Crozet Archipelago. The eastern islands, East and Possession, preferentially sample the E–P component, whereas Penguins Island mainly samples the FOZO component. The scatter in the data is caused by the contribution of a third component, which is likely to be the local DMM. The involvement of a depleted source is confirmed by the relationship between La/Yb and $^{143}Nd/^{144}Nd$ (Fig. 7A, C): lower La/Yb ratios, i.e. higher degree of partial melting, are associated with higher $^{143}Nd/^{144}Nd$ values, i.e. greater contribution of an isotopically more depleted component (DMM-like) (Stracke and Bourdon, 2009).

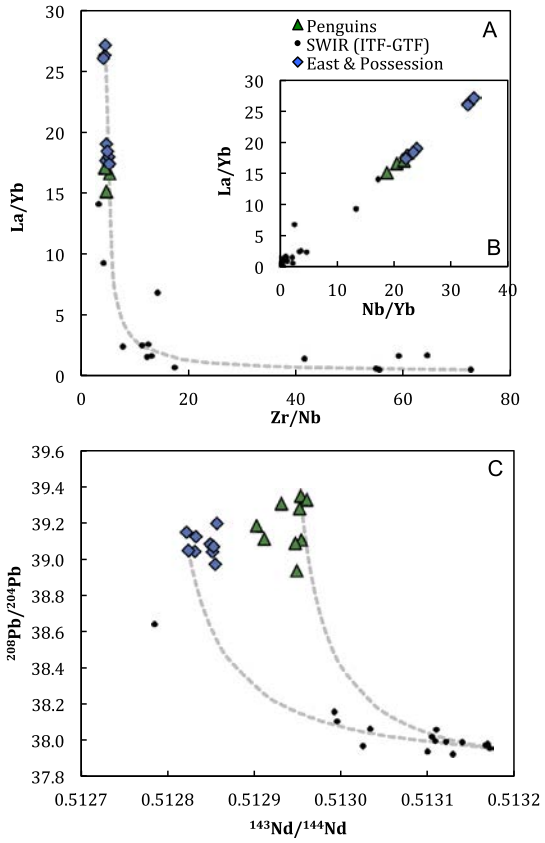

Fig. 7. A – La/Yb vs. Zr/Nb and its companion plot **B** – La/Yb vs. Nb/Yb (Langmuir et al., 1978). Note that the mixing line calculated from the two extreme data points is a good approximation of the hyperbola defined by the Crozet Archipelago and the SWIR section between ITF and GTF. In the companion plot, the hyperbola becomes a linear array, as predicted by Langmuir et al. (1978) for mixings. **C** – The isotopic record ($^{208}Pb/^{204}Pb$ vs. $^{143}Nd/^{144}Nd$) enables to distinguish the three end-members previously identified. The mixing hyperbola calculated between the most extreme MORB value and the two groups of islands also fit the data of the SWIR section between ITF and GTF. Data for the SWIR are from PetDB (references listed in Appendix A4).

Isotope variability within plume products was also observed in other plumes, like Hawaii for example, and sometimes enabled to understand the plume structure and its temporal evolution (Abouchami et al., 2000; Blichert-Toft and Albarède, 2009; Eisele et al., 2003; Fekiacova et al., 2007). We did not perform such an investigation in regard of the limited dataset and the absence of clear temporal relationships between our samples.

5.3. Interaction with the Southwest Indian Ridge

Mid-ocean ridges can locally be influenced by plumes, which modify the bathymetry, morphology and geochemistry along the ridge (Dyment et al., 2007; Schilling 1985, 1986). The SWIR presents important along-axis geophysical and geochemical variations, which are often interpreted as reflecting the influence of hotspots like Bouvet or Marion (Georgen and Lin, 2003; Georgen et al., 2001; Janney et al., 2005; Mahoney et al., 1992).

The segment between the Indomed (ITF, 46°E) and Gallieni (GTF, 52°20′E) transform faults (Fig. 1B) presents evidences of plume–ridge interaction. In particular, the ITF–GTF segment has a low Mantle Bouguer Anomaly and presents an excess of volcanism, which is interpreted as reflecting an interaction with the Crozet hotspot (Georgen and Lin, 2003; Sauter et al., 2009). However, SWIR MORBs between these two transform faults do not show significant shifts in their isotope signatures that could be attributed to the direct influence of a plume, i.e. high $^{87}Sr/^{86}Sr$, $^{206}Pb/^{204}Pb$, $^{207}Pb/^{204}Pb$, $^{208}Pb/^{204}Pb$ and low $^{143}Nd/^{144}Nd$ (Janney et al., 2005; Mahoney et al., 1992; Meyzen et al., 2005). Still, Sauter et al. (2009) attributes the excess of volcanic output in this region and the associated large positive He (R/R_a) anomaly (Gautheron et al., 2008), at 50°E, in-between the ITF and GTF, to the influence of the Crozet plume. The He spike is correlated to increased values in enrichment proxies such as K/Ti and La/Sm (Gautheron et al., 2008). Pb, Sr and Nd anomalies are also observed near the ITF ((Meyzen et al., 2007), 2005), and the presence of a component similar to FOZO is invoked to explain part of the SWIR signature.

Thus two hypotheses could explain these observations: (1) a local contamination of the mantle below the SWIR between ITF and GTF by plume-derived material or (2) a direct plume–ridge interaction that would generate a thermal anomaly and an input of enriched-material to the mantle below the SWIR. However the second hypothesis seems less likely because of the high K/Ti and La/Sm ratios (Gautheron et al., 2008) that suggest a low degree of partial melting. In addition, the positive correlation between these ratios and the R/R_a suggests preferential melting of mantle areas that were re-enriched by plume-derived material.

Consequently, the enriched section of the SWIR between ITF and GTF is likely to be associated to a more fertile mantle below this section of the ridge. We propose that the enrichment characteristics of the ITF–GTF segment results from a ternary mixing that involves the three components identified in the Crozet lavas: the "East–Possession" component, the FOZO component, and the DMM component. The latter component is the most extensively sampled by the SWIR in this region. Two hypotheses may explain the enriched signatures observed along the ITF–GTF section of the SWIR: (1) the Crozet plume is divided in satellite plumes, one of which, at least, reaches the surface near the SWIR (Sauter et al., 2009), or (2) the upper SWIR mantle was previously contaminated by material derived from the Crozet plume. A similar mechanism of contamination of the shallow mantle below the south-eastern Indian Ocean by the Kerguelen plume has been proposed by Storey et al. (1992). This type of mechanism, involving a contamination of the shallow mantle by the Crozet plume could explain the similarities between the Crozet and Reunion basalts and the heterogeneous signatures of the ITF–GTF segment.

In order to check whether the SWIR MORBs of the ITF–GTF segment could result from the mixing between Crozet material and the local DMM, we used incompatible trace element (La, Yb, Zr, Nb) ratios and isotope ratios (Fig. 7). Indeed, the data from Crozet and the SWIR MORBs from the ITF–GTF segment plot along the mixing curves calculated between Crozet basalts (either E162 or OVPG-13) and a MORB from the ITF–GTF segment of the SWIR. We used the basalts with the most extreme compositions as end-members. As Crozet basalts have two different sources, we considered either an East–Possession end-member (E162) or a Penguins end-member (OVPG-13, close to the FOZO-like source) to calculate the two extreme mixing curves (Fig. 7). These two curves are undistinguishable in the La/Yb vs. Zr/Nb plot (Fig. 7A). The mixing hypothesis is supported by the companion plot Fig. 7B, in which the samples resulting from the mixing of the same two components plot along a line (Langmuir et al., 1978). These results clearly show an influence of Crozet material on the MORBs from the ITF–GTF segment of the SWIR. However, trace elements ratios do not allow us to distinguish between a mixing between two or three end-members because East, Possession and Penguins Islands have similar Zr/Nb signatures. Similarly, although the East–Possession group and the Penguins group have distinct isotopic signatures, Fig. 7C show that the signature of the MORBs can be explained either by a binary mixing between the local DMM and one of the two Crozet deep-mantle sources or by a ternary mixing.

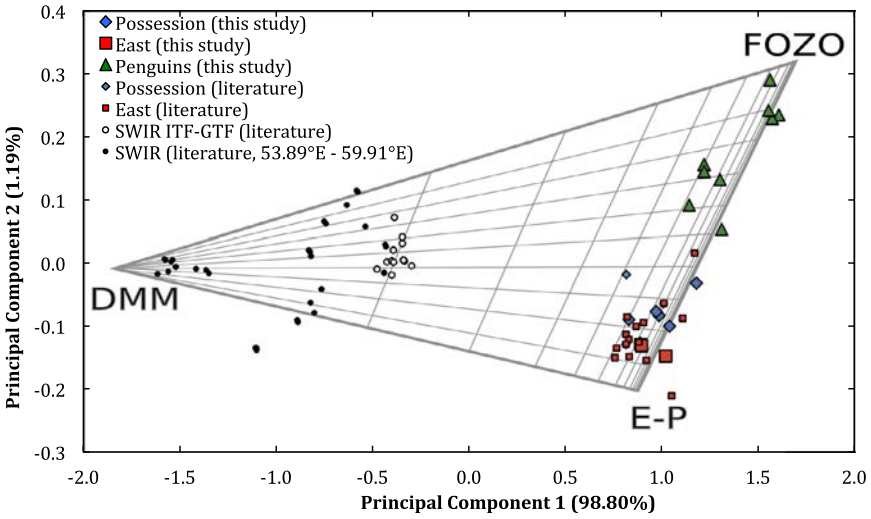

Fig. 8. Principal Component Analysis (PCA) of the $^{206}Pb/^{204}Pb$, $^{207}Pb/^{204}Pb$, $^{208}Pb/^{204}Pb$ data. The first principal component explains 98.80% of the total variability of the data, and the second principal component explains 1.19% of this variability. Hence, this 2D representation of the 3D dataset shows 99.99% of the total variability. The triangular pattern defined by the samples in this diagram is consistent with the proposed ternary mixing between FOZO, E–P and the SWIR DMM. The details of the calculation are given in Appendix A3.

To distinguish between a binary and a ternary mixing, we used a PCA of the Pb isotopic compositions of the Crozet samples and the MORBs from the ITF–GTF segment of the SWIR (Fig. 8 and Appendix A3). The PCA shows that 99.99% of the variance is accounted for by the first two principal components (98.80% by the first principal component). This means the Pb data are located on a plane in the 3D $^{206}Pb/^{204}Pb$ vs. $^{207}Pb/^{204}Pb$ vs. $^{208}Pb/^{204}Pb$ space. In Fig. 8, the data are orthogonally projected on this plane which is defined by the two principal components. MORBs from the ITF–GTF segment are more radiogenic than the uninfluenced lavas from the neighboring segments, i.e. from the Gallieni to the Atlantis II transform faults. MORBs from the ITF–GTF segment likely represent a ternary mixing, as they do not plot along a line but rather in the triangle defined by the three mantle end-members defined for Crozet (see Section 5.2). The influence of the Crozet plume on the SWIR is not localized on a specific section of the ITF–GTF segment contrary to what is observed for the hotspot of the Amsterdam/Saint-Paul Islands (Nicolaysen et al., 2007) which are closer to the ridge than the Crozet hotspot. Rather, the Crozet plume appears to influence the entire ITF–GTF segment, thus its isotopic signature is less pronounced than what is observed for other plume–ridge interactions. We suggest that the upper mantle below the SWIR along the ITF–GTF segment is contaminated by Crozet plume-derived material. This hypothesis is supported by the S-wave anomaly observed below this section of the SWIR and which has been ascribed to the presence of material hotter than the common depleted upper mantle (Sauter et al., 2009). This deep fertile material is sampled in small amounts when the shallower DMM experiences partial melting during oceanic expansion.

6. Conclusions

The geochemical variability observed among the Crozet basalts is the expression of two main processes. The variations in terms of major and trace element concentrations comes from the accumulation/removal of olivine and clinopyroxene to the parental magma, while the variations in isotope ratios and trace elements ratios is due to the heterogeneity of the deep material feeding the Crozet hotspot.

We have shown that the Crozet basalts are heterogeneous in terms of both concentrations of major and trace elements, and isotopic compositions, contrary to what was previously observed. The variations of abundance in trace elements can be accounted for by simple accumulation of olivine and clinopyroxene phenocrysts.

Our new isotope data show that the Crozet hotspot is geochemically heterogeneous. Two groups of lavas can be individualized based on the isotopic data: East and Possession lavas and Penguins lavas. Three mantle sources are required to fully explain the variability within the Crozet basalts: (1) a FOZO-like source that is mainly expressed in Penguins Island lavas, with high R/R_a and $^{143}Nd/^{144}Nd$, low $^{87}Sr/^{86}Sr$, and radiogenic Pb ratios, (2) a source called E–P component that is mainly expressed in East and Possession Islands lavas, with isotopic compositions similar to that of Reunion and Mauritius Islands, and (3) a DMM-like source.

We also show that there is an interaction between material derived from the Crozet plume and the SWIR. The interaction extends over the entire segment of the SWIR located between the Indomed and Gallieni transform faults (46°E and 52°20'E). The high ^{3}He signature of MORB from this section may reflect a contribution of the high ^{3}He signature ($R/R_a > 13$) measured in olivine collected from lavas of Penguins Island. Moreover, mixing between the FOZO-like, DMM and E–P components unambiguously characterize the samples from this section of the SWIR. The plume–ridge interaction is much more diffuse than those observed for hotspots located closer to the ridge, e.g. Saint-Paul/Amsterdam. We propose that the upper mantle located below the ITF–GTF section of the SWIR is contaminated by deep material associated with the Crozet plume.

Acknowledgements

We thank the French Polar Institute (IPEV–DyLioker 444 program) for their support for the sampling, and R. Bellec, N. Leviavant and H. Perau (IPEV staff) for their assistance in the field. We also thank A. Giret and the French Polar Rocks Collection at the Jean Monnet University (Saint-Etienne, France) who provided the samples from Penguins and East Islands. We thank J.-L. Devidal for support during EMP analysis, C. Douchet, E. Albalat, F. Arnaud-Godet, and P. Telouk for maintaining the clean lab and ICP-MS facilities in Lyon in state-of-the-art working conditions. We thank P. Bowden, G. Quitté and K.T. Koga who kindly accepted to proofread early versions of the manuscript. Thoughtful and constructive reviews by Andreas Stracke and three anonymous reviewers improved the manuscript considerably. Authors acknowledge the

support of “ClerVolc program” (this is Laboratory of Excellence ClerVolc contribution no. 63).

References

Abouchami, W., Galer, S.J.G., Hofmann, A.W., 2000. High precision lead isotope systematics of lavas from the Hawaiian Scientific Drilling Project. Chem. Geol. 169, 187–209.

Blichert-Toft, J., Albarède, F., 2009. Mixing of isotopic heterogeneities in the Mauna Kea plume conduit. Earth Planet. Sci. Lett. 282, 190–200.

Cantagrel, J.M., Lameyre, J., Nougier, J., 1980. Volcanologie et géochronologie d'une île volcanique, île de l'Est (archipel Crozet). In: 26th Intern. Geol. Congress, Abstracts, pp. 26–27.

Chevallier, L., Nougier, J., 1981. Première étude volcano-structurale de l'île de la Possession, îles Crozet (TAAF). C. R. Acad. Sci. Paris 292, 363–368.

Dupré, B., Allègre, C.J., 1983. Pb–Sr isotope variation in Indian Ocean basalts and mixing phenomena. Nature 303, 142–146.

Dyment, J., Lin, J., Baker, E.T., 2007. Ridge–hotspot interactions: What mid-ocean ridges tell us about deep earth processes. Oceanography 20, 102–115.

Eisele, J., Abouchami, W., Galer, S.J.G., Hofmann, A.W., 2003. The 320 kyr Pb isotope evolution of Mauna Kea lavas recorded in the HSDP-2 drill core. Geochem. Geophys. Geosyst. 4.

Farley, K.A., Neroda, E., 1998. Noble gases in the Earth's mantle. Annu. Rev. Earth Planet. Sci. 26, 189–218.

Farley, K.A., Natland, J.H., Craig, H., 1992. Binary mixing of enriched and undegassed (primitive?) mantle components (He, Sr, Nd, Pb) in Samoan lavas. Earth Planet. Sci. Lett. 111, 183–199.

Fekiacova, Z., Abouchami, W., Galer, S.J.G., Garcia, M.O., Hofmann, A.W., 2007. Origin and temporal evolution of Ko'olau Volcano, Hawai'i: Inferences from isotope data on the Ko'olau Scientific Drilling Project (KSDP), the Honolulu Volcanics and ODP Site 843. Earth Planet. Sci. Lett. 261, 65–83.

Galer, S.J.G., Abouchami, W., 1998. Practical application of lead triple spiking for correction of instrumental mass discrimination. Mineral. Mag. 62A, 491–492.

Gautheron, C.E., Bézos, A., Moreira, M., Humler, E., 2008. Helium and Trace Element Geochemical Signals in the Southwest Indian Ocean. Goldschmidt Conference Abstracts. Geochim. Cosmochim. Acta 72, A300.

Georgen, J.E., Lin, J., 2003. Plume-transform interactions at ultra-slow spreading ridges: Implications for the Southwest Indian Ridge. Geochem. Geophys. Geosyst. 4.

Georgen, J.E., Lin, J., Dick, H.J.B., 2001. Evidence from gravity anomalies for interactions of the Marion and Bouvet hotspots with the Southwest Indian Ridge: Effects of transform offsets. Earth Planet. Sci. Lett. 187, 283–300.

Giret, A., Tourpin, S., Marc, S., Verdier, O., Cottin, J.Y., 2002. Penguins Island, Crozet Archipelago, volcanic evidence for a heterogeneous mantle in the southern Indian Ocean. C. R. Acad. Sci. Paris 334, 481–488.

Giret, A., Weis, D., Zhou, X., Cottin, J.-Y., Tourpin, S., 2003. Géologie des îles Crozet. Géologues 137, 15–23.

Goslin, J., Patriat, P., 1984. Absolute and relative plate motions and hypotheses on the origin of five aseismic ridges in the Indian Ocean. Tectonophysics 101, 221–244.

Goslin, J., Recq, M., Schlich, R., 1981. Emplacement and evolution of the Madagascar ridge and Crozet submarine Plateau. Bull. Soc. Geol. Fr. 23, 609–618.

Graham, D., Lupton, J., Albarède, F., Condomines, M., 1990. Extreme temporal homogeneity of helium isotopes at Piton de la Fournaise, Réunion Island. Nature 347, 545–548.

Gunn, B.M., Coyyll, R., Watkins, N.D., Abranson, C.E., Nougier, J., 1970. Geochemistry of an oceanite–ankaramite–basalt suite from East Island, Crozet Archipelago. Contrib. Mineral. Petrol. 28, 319–339.

Halliday, A.N., Lee, D.C., Tommasini, S., Davies, G.R., Paslick, C.R., Fitton, J.G., James, D.E., 1995. Incompatible trace elements in OIB and MORB and source enrichment in the sub-oceanic mantle. Earth Planet. Sci. Lett. 133, 379–395.

Hanan, B.B., Graham, D.W., 1996. Lead and helium isotope evidence from oceanic basalts for a common deep source of mantle plumes. Science 272, 991–995.

Hart, S.R., Hauri, E.H., Oschmann, L.A., Whitehead, J.A., 1992. Mantle plumes and entrainment – isotopic evidence. Science 256, 517–520.

Hedge, C.E., Watkins, N.D., Hildreth, R.A., Doering, W.P., 1973. $^{87}Sr/^{86}Sr$ ratios in basalts from islands in Indian Ocean. Earth Planet. Sci. Lett. 21, 29–34.

Hofmann, A.W., 1988. Chemical differentiation of the Earth: The relationship between mantle, continental crust, and oceanic crust. Earth Planet. Sci. Lett. 90, 297–314.

Hofmann, A.W., 2007. Sampling mantle heterogeneity through oceanic basalts: Isotopes and trace elements. In: Heinrich, D.H., Karl, K.T. (Eds.), Treatise on Geochemistry. Pergamon, Oxford, pp. 1–44.

Hofmann, A.W., Jochum, K.P., Seufert, M., White, W.M., 1986. Nb and Pb in oceanic basalts: new constraints on mantle evolution. Earth Planet. Sci. Lett. 79, 33–45.

Hofmann, A.W., Farnetani, C.G., Spiegelman, M., Class, C., 2011. Displaced helium and carbon in the Hawaiian plume. Earth Planet. Sci. Lett. 312, 226–236.

Hopp, J., Trieloff, M., 2005. Refining the noble gas record of the Réunion mantle plume source: Implications on mantle geochemistry. Earth Planet. Sci. Lett. 240, 573–588.

Janney, P.E., Le Roex, A.P., Carlson, R.W., 2005. Hafnium isotope and trace element constraints on the nature of mantle heterogeneity beneath the central Southwest Indian Ridge (13°E to 47°E). J. Petrol. 46, 2427–2464.

Lameyre, J., Nougier, J., 1982. Geology of Ile de l'Est, Crozet Archipelago (TAAF). In: Cradock, C. (Ed.), Antarctic Geoscience. The University of Wisconsin Press, Madison, pp. 767–770.

Langmuir, C.H., Vocke, R.D., Hanson, G.N., Hart, S.R., 1978. A general mixing equation with applications to Icelandic basalts. Earth Planet. Sci. Lett. 37, 380–392.

Le Maitre, R.W., Bateman, P., Dudek, A., Keller, J., Lameyre, J., Le Bas, M.P., Sabine, P.A., Schmid, R., Sorensen, H., Streckeisen, A., Wolley, A.R., Zannetin, B., 1989. A classification of igneous rocks and glossary of terms. Blackwell Scientific Publ..

Le Roex, A.P., Dick, H.J.B., Fisher, R.L.., 1989. Petrology and geochemistry of MORB from 25°E to 46°E along the Southwest Indian Ridge: Evidence for contrasting styles of mantle enrichment. J. Petrol. 30, 947–986.

Le Roex, A.P., Chevallier, L., Verwoerd, W.J., Barends, R., 2012. Petrology and geochemistry of Marion and Prince Edward Islands, Southern Ocean: Magma chamber processes and source region characteristics. J. Vulcanol. Geothermal Res. 223–224, 11–28.

LeMasurier, W., Thomson, J.W., Baker, P., Kyle, P., Rowley, J., Smellie, J., Verwoerd, W.J., 1990. Volcanoes of the Antarctic Plate and Southern Oceans. Antarct. Res. Ser. 48, 487 pp.

Lugmair, G.W., Galer, S.J.G., 1992. Age and isotopic relationships among the angrites Lewis Cliff 86010 and Angra Dos Reis. Geochim. Cosmochim. Acta 56, 1673–1694.

Mahoney, J., Le Roex, A.P., Peng, Z., Fisher, R.L., Natland, J.H., 1992. Southwestern limits of Indian Ocean Ridge mantle and the origin of low $^{206}Pb/^{204}Pb$ mid-ocean ridge basalt: Isotope systematics of the central Southwest Indian Ridge (17°–50°E). J. Geophys. Res., Solid Earth 97, 19771–19790.

Mahoney, J.J., White, W.M., Upton, B.G.J., Neal, C.R., Scrutton, R.A., 1996. Beyond EM-1: Lavas from Afanasy-Nikitin Rise and the Crozet Archipelago, Indian Ocean. Geology 24, 615–618.

Meyzen, C.M., Ludden, J.N., Humler, E., Luais, B., Toplis, M.J., Mével, C., Storey, M., 2005. New insights into the origin and distribution of the DUPAL isotope anomaly in the Indian Ocean mantle from MORB of the Southwest Indian Ridge. Geochem. Geophys. Geosyst. 6.

Meyzen, C.M., Blichert-Toft, J., Ludden, J.N., Humler, E., Mével, C., Albarède, F., 2007. Isotopic portrayal of the Earth's upper mantle flow field. Nature 447, 1069–1074.

Montelli, R., Nolet, G., Dahlen, F.A., Masters, G., Engdahl, E.R., Hung, S.H., 2004. Finite-frequency tomography reveals a variety of plumes in the mantle. Science 303, 338–343.

Montelli, R., Nolet, G., Dahlen, F.A., Masters, G., 2006. A catalogue of deep mantle plumes: New results from finite-frequency tomography. Geochem. Geophys. Geosyst. 7.

Moreira, M., Staudacher, T., Sarda, P., Schilling, J.G., Allègre, C.J., 1995. A primitive plume neon component in MORB: The Shona Ridge anomaly, South Atlantic (51–52°S). Earth Planet. Sci. Lett. 133, 367–377.

Nicolaysen, K.P., Frey, F.A., Mahoney, J.J., Johnson, K.T.M., Graham, D.W., 2007. Influence of the Amsterdam/St. Paul hot spot along the Southeast Indian Ridge between 77° and 88°E: Correlations of Sr, Nd, Pb, and He isotopic variations with ridge segmentation. Geochem. Geophys. Geosyst. 8.

Pin, C., Bassin, C., 1992. Evaluation of a strontium-specific extraction chromatographic method for isotopic analysis in geological materials. Anal. Chim. Acta 269, 249–255.

Pin, C., Briot, D., Bassin, C., Poitrasson, F., 1994. Concomitant separation of strontium and samarium–neodymium for isotopic analysis in silicate samples, based on specific extraction chromatography. Anal. Chim. Acta 298, 209–217.

Recq, M., Goslin, J., Charvis, P., Operto, S., 1998. Small-scale crustal variability within an intraplate structure: the Crozet Bank (Southern Indian Ocean). Geophys. J. Int. 134, 145–156.

Ryan, W.B.F., Carbotte, S.M., Coplan, J.O., O'Hara, S., Melkonian, A., Arko, R., Weissel, R.A., Ferrini, V., Goodwillie, A., Nitsche, F., Bonczkowski, J., Zemsky, R., 2009. Global multi-resolution topography synthesis. Geochem. Geophys. Geosyst. 10.

Salters, V.J.M., White, W.M., 1998. Hf isotope constraints on mantle evolution. Chem. Geol. 145, 447–460.

Sauter, D., Cannat, M., Meyzen, C., Bezos, A., Patriat, P., Humler, E., Debayle, E., 2009. Propagation of a melting anomaly along the ultraslow Southwest Indian Ridge between 46°E and 52°20'E: interaction with the Crozet hotspot? Geophys. J. Int. 179, 687–699.

Schilling, J.G., 1985. Upper mantle heterogeneities and dynamics. Nature 314, 62–67.

Schilling, J.G., 1986. Geochemical and isotopic variation along the Mid-Atlantic Ridge axis from 79°N to 0°N. In: Vogt, P.R., Tucholke, B.E. (Eds.), The Western North Atlantic Region. Geological Society of America, pp. 137–156.

Schilling, J.G., 1991. Fluxes and excess temperatures of mantle plumes inferred from their interaction with migrating mid-ocean ridges. Nature 352, 397–403.

Storey, M., Kent, R., Saunders, A.D., Salters, V.J., Hergt, J., Whitechurch, H., Thirwall, M.F., Leat, P., Ghose, N.C., Gifford, M., 1992. Lower Cretaceous volcanic rocks along continental margins and their relationship to the Kerguelen Plateau. Proc. ODP, Sci. Res., 33–53.

Stracke, A., Bourdon, B., 2009. The importance of melt extraction for tracing mantle heterogeneity. Geochim. Cosmochim. Acta 73, 218–238.

Stracke, A., Hofmann, A.W., Hart, S.R., 2005. FOZO, HIMU, and the rest of the mantle zoo. Geochem. Geophys. Geosyst. 6.

van der Hilst, R.D., de Hoop, M.V., 2005. Banana-doughnut kernels and mantle tomography. Geophys. J. Int. 163, 956–961.

Vollmer, R., 1976. Rb–Sr and U–Th–Pb systematics of alkaline rocks: the alkaline rocks from Italy. Geochim. Cosmochim. Acta 40, 283–295.

White, W.M., Albarède, F., Telouk, P., 2000. High-precision analysis of Pb isotope ratios by multi-collector ICP-MS. Chem. Geol. 167, 257–270.

Workman, R.K., Hart, S.R., 2005. Major and trace element composition of the depleted MORB mantle (DMM). Earth Planet. Sci. Lett. 231, 53–72.

Zhou, X., 1996. Ile de l'Est (Crozet archipelago, Southwestern Indian Ocean); Petrogenesis of the plutonic complexes. Université libre de Bruxelles, Bruxelles.